2018

A cell-intrinsic interferon-like response links replication stress to cellular aging caused by progerin

Ray Kreienkamp
Saint Louis University School of Medicine

Simona Graziano
Saint Louis University School of Medicine

Nuria Coll-Bonfill
Saint Louis University School of Medicine

Gonzalo Bedia-Diaz
Saint Louis University School of Medicine

Emily Cybulla
Saint Louis University School of Medicine

See next page for additional authors

Cell Reports

Report

A Cell-Intrinsic Interferon-like Response Links Replication Stress to Cellular Aging Caused by Progerin

Graphical Abstract

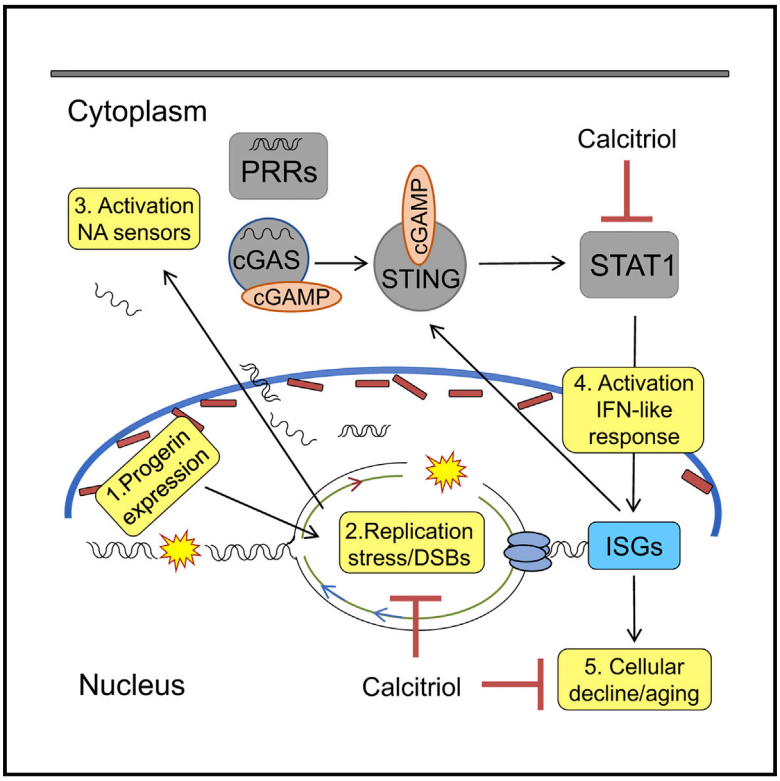

Highlights

- Replication stress in progerin-expressing cells is caused by fork stalling and degradation
- Progerin activates cGAS/STING pathway and a robust STAT1-regulated IFN-like response
- Replication stress and IFN-like response contribute to HGPS cellular aging phenotypes
- Calcitriol reduces replication stress and IFN-like response, rejuvenating HGPS cells

Authors

Ray Kreienkamp, Simona Graziano, Nuria Coll-Bonfill, ..., Nard Kubben, Luis Francisco Zirnberger Batista, Susana Gonzalo

Correspondence

sgonzalo@slu.edu

In Brief

Kreienkamp et al. reveal mechanisms underlying cellular decline in the premature aging disease Hutchinson-Gilford progeria syndrome. Progerin, the mutant protein that causes this disease, elicits replication stress and a cell-intrinsic innate immune response. The study identifies strategies, such as calcitriol, that rescue these phenotypes and rejuvenate progeria cells.

Data and Software Availability

GSE97986

Kreienkamp et al., 2018, Cell Reports 22, 2006–2015
February 20, 2018
https://doi.org/10.1016/j.celrep.2018.01.090

CellPress

OPEN ACCESS
CellPress

Cell Reports
Report

A Cell-Intrinsic Interferon-like Response Links Replication Stress to Cellular Aging Caused by Progerin

Ray Kreienkamp,[1,4] Simona Graziano,[1,4] Nuria Coll-Bonfill,[1,4] Gonzalo Bedia-Diaz,[1] Emily Cybulla,[1] Alessandro Vindigni,[1] Dale Dorsett,[1] Nard Kubben,[3] Luis Francisco Zirnberger Batista,[2] and Susana Gonzalo[1,5,*]

[1]Edward A. Doisy Department of Biochemistry and Molecular Biology, St. Louis University School of Medicine, 1100 S. Grand Blvd., St. Louis, MO 63104, USA

[2]Departments of Medicine and Developmental Biology, Washington University, 660 S. Euclid Ave., St. Louis, MO 63110, USA

[3]National Cancer Institute, NIH, Bethesda, MD 20892, USA

[4]These authors contributed equally

[5]Lead Contact

*Correspondence: sgonzalo@slu.edu

https://doi.org/10.1016/j.celrep.2018.01.090

SUMMARY

Hutchinson-Gilford progeria syndrome (HGPS) is a premature aging disease caused by a truncated lamin A protein (progerin) that drives cellular and organismal decline. HGPS patient-derived fibroblasts accumulate genomic instability, but its underlying mechanisms and contribution to disease remain poorly understood. Here, we show that progerin-induced replication stress (RS) drives genomic instability by eliciting replication fork (RF) stalling and nuclease-mediated degradation. Rampant RS is accompanied by upregulation of the cGAS/STING cytosolic DNA sensing pathway and activation of a robust STAT1-regulated interferon (IFN)-like response. Reducing RS and the IFN-like response, especially with calcitriol, improves the fitness of progeria cells and increases the efficiency of cellular reprogramming. Importantly, other compounds that improve HGPS phenotypes reduce RS and the IFN-like response. Our study reveals mechanisms underlying progerin toxicity, including RS-induced genomic instability and activation of IFN-like responses, and their relevance for cellular decline in HGPS.

INTRODUCTION

A-type lamins (lamin A/C), nuclear structural components, provide a scaffold for the compartmentalization of genome function (van Steensel and Belmont, 2017). *LMNA* gene mutations are associated with degenerative disorders termed laminopathies, including Hutchinson-Gilford progeria syndrome (HGPS), a premature aging disease that causes patients death in their teens from cardiovascular disease (CVD) (Gordon et al., 2014; Pereira et al., 2008). Since HGPS was genetically mapped, we have made major strides understanding its pathology and identified therapies that ameliorate disease in mouse models (Gonzalo et al., 2016). However, we still lack strategies to ameliorate disease progression in patients, because of the extensive toxic effects of progerin, including disruption of nuclear architecture, and genome stability and function. The current view is that key mechanisms behind progerin-induced cellular and organismal aging remain to be discovered.

Extensive evidence links progerin expression with DNA repair deficiencies and telomere dysfunction (Cao et al., 2011a; Chojnowski et al., 2015; Gonzalo and Kreienkamp, 2015). Although replication stress (RS) is a major contributor to genomic instability, having serious implications for cell survival and human disease, how progerin affects DNA replication has been minimally explored. Studies suggest that lamins are required for restart of stalled replication forks (RFs) (Singh et al., 2013) and that progerin disrupts PCNA/lamin A interactions by sequestering PCNA away from the RF (Cobb et al., 2016; Hilton et al., 2017; Wheaton et al., 2017). However, the mechanisms whereby progerin causes RS and the consequences for progeria cellular fitness remain unknown.

The concept is emerging that DNA damage and RS not only underlie the genomic instability that drives aging and cancer but also contribute to activate inflammatory responses that facilitate malignancy in some cases and senescence in others (Brzostek-Racine et al., 2011; Härtlova et al., 2015; Yu et al., 2015). For instance, RS leads to accumulation of self-nucleic acids in the cytoplasm that are erroneously recognized as foreign by pattern recognition receptors (PRRs), proteins that survey the extracellular and cytoplasmic space for the presence of pathogens, activating immune responses (Ahn et al., 2014; Bhattacharya et al., 2017; Wolf et al., 2016). In particular, the cGAS/STING cytosolic DNA sensing pathway is critical for activating interferon (IFN) responses (Vincent et al., 2017) and has been implicated in neoplasia (Mackenzie et al., 2017; Wang et al., 2017) and senescence (Yang et al., 2017).

Here, we show that progerin elicits RF stalling and nuclease-mediated fork degradation, revealing a mechanism underlying DNA damage accumulation in HGPS. RS is accompanied by upregulation of the cGAS/STING pathway and activation of a robust STAT1-regulated IFN-like response. Moreover, we demonstrate that reduction of RS and the IFN-like response

improves HGPS cellular fitness, suggesting a role for these pathways in progerin-induced pathology.

RESULTS

Progerin Expression Causes RF Stalling and Degradation

To determine how progerin affects DNA replication, we performed single-molecule replication analysis (DNA fiber assays) in retinal pigment epithelial (RPE) cells lentivirally transduced with progerin or empty vector (EV) (Figure 1A). We labeled replication events with the thymidine analogs iododeoxyuridine (IdU) and chlorodeoxyuridine (CldU), measured individual IdU and CldU tract lengths, and calculated the CldU/IdU ratio. In control cells (EV), the CldU/IdU ratio is ~1, consistent with normal RF progression. Progerin expression causes shortening of CldU tract length and thus decreased CldU/IdU ratio (Figure 1A), as well as increased frequency of stalled forks (Figure 1B). Importantly, overexpression of lamin A protein did not cause replication defects (Figure 1C). To determine if tract shortening upon progerin expression is due to fork deprotection and nuclease-mediated degradation, we treated cells with mirin, an inhibitor of MRE11 nuclease that attacks deprotected stalled forks (Schlacher et al., 2011). Mirin rescues replication problems (Figure 1D), indicating that progerin causes fork deprotection and degradation. Thus, we demonstrate that progerin perturbs fork progression, causing RS. Given our findings that calcitriol reduces DNA damage in HGPS cells (Kreienkamp et al., 2016), we tested if it ameliorates RS in progerin-expressing cells. We find that the reduced ratio CldU/IdU in progerin-expressing cells is normalized by calcitriol (Figure 1E). This indicates that calcitriol rescues RS, providing a mechanism behind the effects of calcitriol ameliorating DNA damage in HGPS cells. Accordingly, HGPS fibroblasts show high levels of phosphorylated RPA (P-RPA), a marker of single-stranded DNA (ssDNA) associated with RS and DNA damage (Murphy et al., 2014), which is reduced by calcitriol (Figure 1F).

Activation of an IFN-like Response in HGPS Cells

DNA damage and RS can activate IFN responses, which in turn can contribute to senescence or malignant transformation (Härtlova et al., 2015; Yu et al., 2015). Interestingly, our genome-wide expression analysis of HGPS cells reveals robust activation of a STAT1-mediated IFN-like response and a marked repression of this response by calcitriol. Figure 2 shows the results of RNA sequencing (RNA-seq) performed in HGPS fibroblasts derived from four patients, and normal fibroblasts (NFs) from three parents, subjected to prolonged (3 months) and short (4 days) treatments with calcitriol or vehicle (Figure 2A). Differential expression was tested between HGPS/NF and HGPScalcitriol/vehicle (short and long treatment combined), and pathway analysis was performed using DAVID and STRING with genes showing a fold change (FC) > 1.5 or < 0.6 and $p \leq 0.05$. Figure 2B shows the main changes in biological processes in the different conditions. Note the upregulation of genes in the IFN/antiviral/innate immunity category in HGPS cells and how calcitriol treatment downregulates genes in this category. Calcitriol also counteracts deregulation of other biological processes, such as extracellular matrix/cell adhesion and the Wnt/β-catenin pathway, previously identified in progerin-expressing cells (Csoka et al., 2004; Scaffidi and Misteli, 2008). A more complete analysis of gene expression changes in NFs and HGPS cells treated with vehicle or calcitriol is shown in Table S1. The heatmap in Figure 2C focuses on the most robust signature, the IFN/antiviral/innate immunity process, with nearly 50 genes in this pathway upregulated in HGPS and downregulated by calcitriol. These include genes encoding for PRRs (RIG-I, MDA5, OASs, and TLR3), PRR effectors (MYD88, IRF1/7/9, STAT1, and NFκB), and more than 40 STAT1-regulated IFN-stimulated genes (ISGs). This signature represents a robust IFN-like response. However, IFNs themselves are not expressed in HGPS fibroblasts, indicating that the upregulation of STAT1 and ISGs is a cell-intrinsic and IFN-independent process. In addition, calcitriol reduces expression of the majority of genes in the PRR/STAT1/IFN-like response that are upregulated in HGPS cells, indicating a robust effect suppressing this pathway.

STAT1-mediated regulation of ISGs contributes to inflammation, especially during atherosclerosis, being an important therapeutic target for CVD (Szelag et al., 2016). STAT1 is activated by phosphorylation on Y701, which promotes its translocation to the nucleus, where it is further phosphorylated on S727, resulting in maximal transcriptional regulation of target genes. This is part of the innate immune response that activates ISGs. Immunofluorescence analysis shows that STAT1 is found in the cytoplasm and the nucleus in NFs, as expected (Figure 2D). HGPS cells show accumulation of STAT1 and P-STAT1^{Y701} in the nucleus, suggesting constitutive STAT1 activation. Importantly, STAT1 is phosphorylated in early passage HGPS cells, and 4-day calcitriol treatment reduces its phosphorylation (Figures 2E and 2G). Subcellular fractionation shows increased levels of nuclear P-STAT1^{Y701} and IRF3 in HGPS cells, which are reduced by calcitriol (Figures 2F and 2G). These data show that HGPS cells activate PRRs and STAT1 and that calcitriol counteracts their activation.

Progerin Expression Activates the cGAS/STING Cytosolic DNA Sensing Pathway and STAT1-Regulated IFN-like Response

To determine if progerin expression is sufficient to activate the STAT1-mediated IFN-like response in normal cells, we transduced BJ fibroblasts with progerin or EV control. As shown in Figures 3A and S1, progerin expression increases markers of DNA damage (γH2AX) and RS (P-RPA), global levels of PRRs, including cGAS and STING (DNA sensors), and RIG-I and OAS1 (RNA sensors), in addition to STAT1 and IRF3. As evidence for the role of STAT1 mediating upregulation of ISGs, reduced expression of STAT1 in HGPS cells with different short hairpin RNAs (shRNAs) reduces expression of *MX1*, *APOBEC3G*, and *IFIT1* (Figure 3B), which are among the most highly upregulated ISGs in HGPS cells. These data demonstrate that progerin activates the cGAS/STING pathway and a STAT1-modulated IFN-like response. To monitor the activation of these pathways upon progerin expression over time, we used human skin-derived fibroblasts (HDF) containing GFP-progerin or GFP-lamin A under the control of doxycycline-inducible (Tet-on) promoters (Figure 3C). Expression of GFP-progerin in these cells

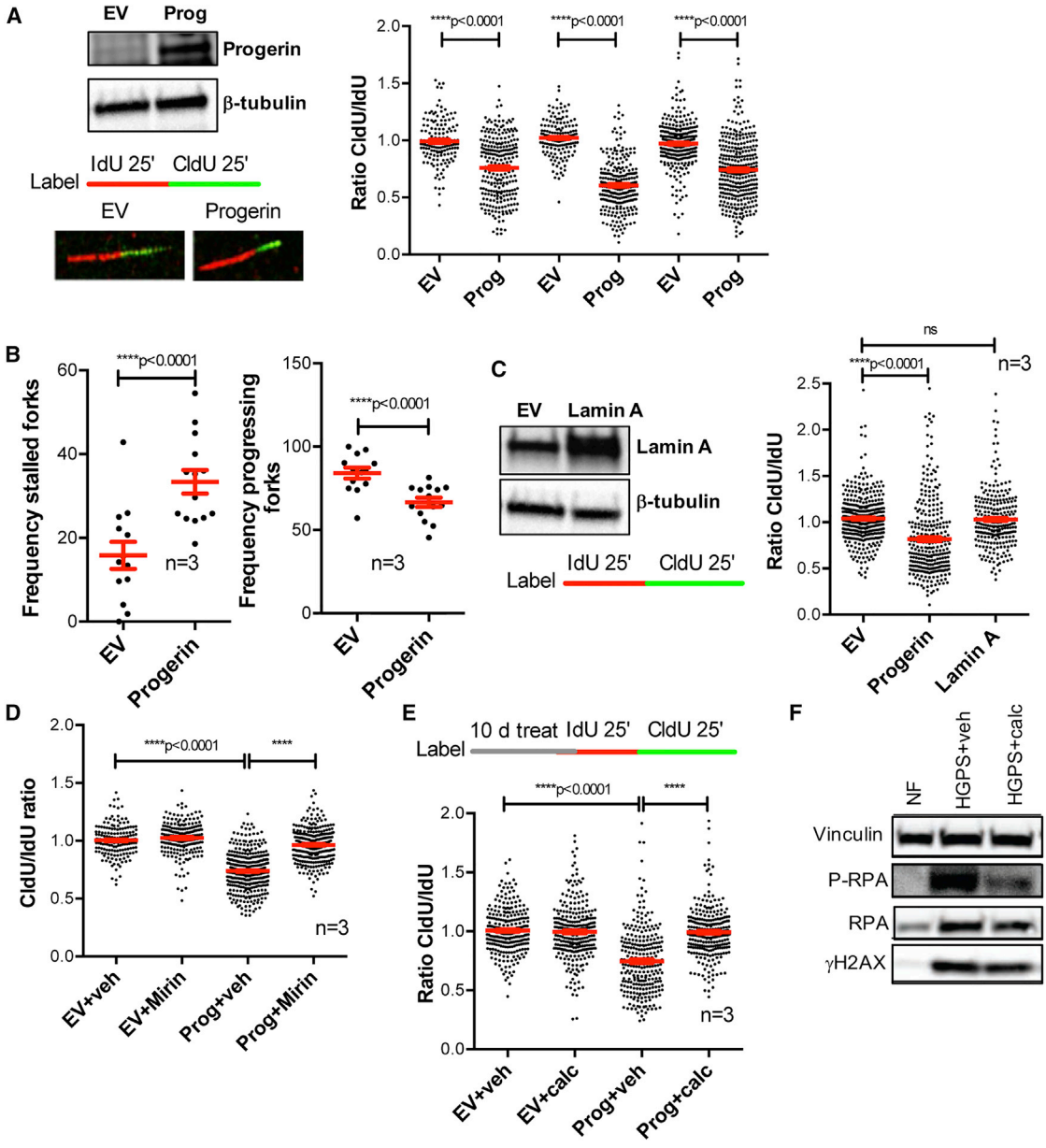

Figure 1. Replication Stress (RS) in Progerin-Expressing Cells

(A) RPE cells were lentivirally transduced with progerin or empty vector (EV), and single-molecule replication analysis was performed. Immunoblots show the expression levels of progerin. Images show the incorporation of thymidine analogs in cells labeled with IdU for 25 min + CldU for 25 min, as detected by fluorescence confocal microscopy. Tract lengths are measured using ImageJ. Graph shows the tract length ratio CldU/IdU, which in control cells is 1 and in progerin-expressing cells is lower, indicating RF progression defects. Each experiment represents a biological repeat, with independent progerin expression. In each experiment, 200–250 forks were measured.

(B) The frequencies of stalled forks (only IdU signal) and progressing forks (both IdU and CldU signals) were counted in the three independent experiments in (A).

(C) DNA fibers were performed in RPE cells transduced with lamin A, progerin, or EV constructs. Graph shows the average ratio CldU/IdU in three biological repeats.

(D) DNA fiber assays performed with the same labeling scheme as in (A) in progerin-expressing and control RPE cells and treated with vehicle or mirin (5 μM) for 3 hr to inhibit Mre11 nuclease.

(E) Progerin-expressing and control RPE cells were treated with calcitriol (100 nM) for 10 days, and DNA fiber assays were performed as in (A).

(F) Untreated NFs and HGPS fibroblasts treated with vehicle or calcitriol for 4 days were processed for immunoblotting to monitor the levels of phosphorylated RPA (P-RPA) and H2AX (γH2AX). Vinculin was used as loading control.

* denotes p value of statistical significance (*p < 0.05, **p < 0.01, ***p < 0.005, and ****p < 0.001). Error bars represent SEM.

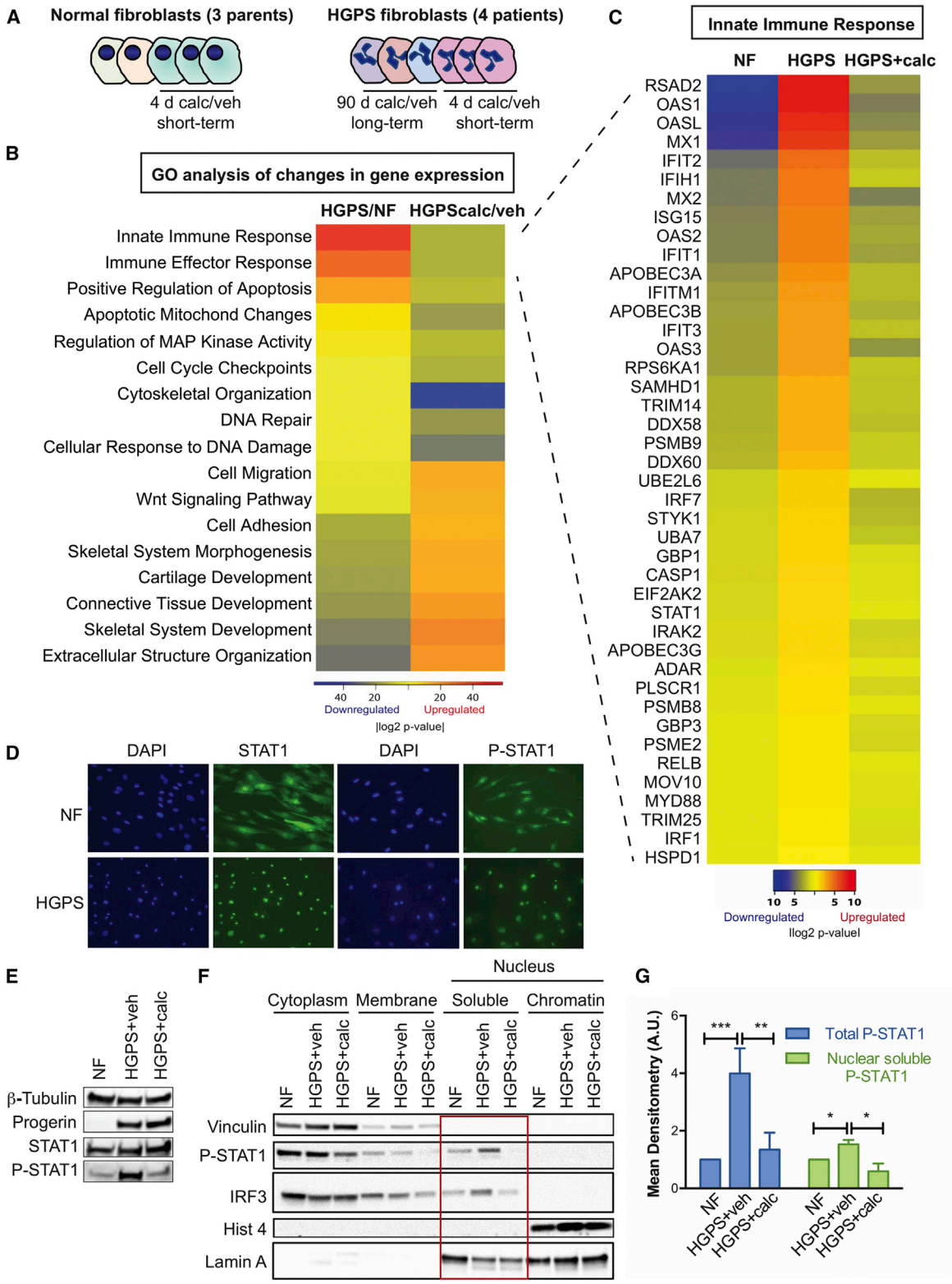

Figure 2. An IFN-like Response in HGPS Fibroblasts is Repressed by Calcitriol

(A) Scheme of the samples analyzed by RNA-seq. NFs derived from three parents of HGPS patients were sequenced. One line of NFs was supplemented with calcitriol (100 nM) or vehicle for 4 days in three biological repeats. HGPS fibroblasts derived from four patients were subjected to prolonged (3 months) and short (4 days) treatments with calcitriol or vehicle. RNA was extracted and sequenced.

(legend continued on next page)

causes nuclear defects, decreased lamin B1 and LAP2 levels, reduced heterochromatic marks, and DNA damage accumulation (Kubben et al., 2016). We find upregulation of cytosolic sensors of DNA (cGAS and STING) and RNA (RIG-I and MDA5), and increased STAT1 phosphorylation 4 days post-induction of GFP-progerin (Figure 3C). In contrast, expression of GFP-lamin A does not upregulate any of these factors (Figure 3C). In addition, progerin elicits upregulation of ISG15, a ubiquitin-like small protein that modifies covalently proteins (ISGylation) upon IFN pathway activation. The upregulation of ISGs (*MX1*, *IFIT3*, and *ISG15*) upon progerin induction was confirmed at the transcript level (Figure 3D). Thus, progerin expression rapidly activates an IFN-like response. Moreover, immortalized adult fibroblasts from a mouse model of HGPS ($Lmna^{G609G/G609G}$ iMAFs) show nuclear accumulation of P-STAT1 (Figure 3E) and increased global levels of γH2AX, P-STAT1, and PRRs (Figure 3F), thus indicating activation of STAT1/IFN signaling also in progerin-expressing mouse cells. Interestingly, progerin-expressing human and mouse cells accumulate difficult-to-replicate domains such as telomeric DNA in the cytoplasm, as shown by immuno-fluorescence in situ hybridization (FISH) performed with lamin A antibody and a PNA-labeled telomere probe (Figure 3G). These data support the notion that cytoplasmic accumulation of nucleic acids due to RS and DNA damage triggers STAT1 activation and an IFN-like response in progerin-expressing cells.

Activation of STAT1-Mediated IFN-like Response Contributes to Progeria Cellular Phenotypes

We postulated that if the pathways identified here contribute to progerin cellular toxicity, treatments known to ameliorate HGPS cellular phenotypes might repress these pathways. These treatments include rapamycin, which increases progerin clearance by autophagy (Cao et al., 2011b); lonafarnib, which inhibits prenylation of progerin (Gordon et al., 2016); retinoids such as ATRA, which repress progerin expression (Kubben et al., 2015; Pellegrini et al., 2015; Swift et al., 2013); and remodelin (Larrieu et al., 2014). We tested how these compounds affect DNA replication and STAT1 activation. Progerin-expressing RPE cells and HGPS fibroblasts were treated with vehicle, calcitriol, ATRA, remodelin, or a combination of lonafarnib and rapamycin for 10 days, as this combination is being tested in a clinical trial for HGPS (Collins, 2016). Interestingly, all these treatments rescue replication problems, as shown by DNA fiber assays (Figure 4A), and reduce the levels of active phosphorylated STAT1 (Figure 4B), although to different extents. Thus, strategies that ameliorate HGPS cellular phenotypes mimic the effect of calcitriol, reducing RS and repressing the STAT1 pathway, though calcitriol's effect is the most robust. Our data suggest that RS and the STAT1/IFN-like response contribute to the decline of HGPS cells. Supporting this notion, the STAT1/IFN pathway is activated in aged normal human fibroblasts and associated with their decreased functionality (proliferation, migration, and differentiation) (Midgley et al., 2016). We generated progerin-expressing fibroblasts knocked down for STAT1 (Figure 4C) and characterized their functionality. We identified shRNAs that when transduced in progerin-expressing cells reduce STAT1 to near normal levels (Figure 4C). STAT1-knockdown (KD) reduces progerin-induced upregulation of RIG-I, STING, and ISG15 (both conjugated and free), as expression of these factors is regulated by STAT1. Consistent with STAT1 anti-proliferative effects in NFs, STAT1-KD increases proliferation in control cells (Figure 4D). Importantly, STAT1-KD restores normal proliferation of progerin-expressing cells, as shown by Ki67 positivity (Figure 4D) and normal migration in a wound closure assay (Figure 4E). These data demonstrate that the STAT1/IFN response contributes to functionality decline of progerin-expressing fibroblasts and suggest that the beneficial effects of calcitriol and other compounds improving HGPS cellular aging phenotypes involve repression of this response.

Hallmarks of aging in HGPS fibroblasts include genomic instability, premature senescence, and low efficiency of reprogramming into induced pluripotent stem cells (iPSCs) (Liu et al., 2011; Zhang et al., 2011). Reprogramming of somatic cells into iPSCs erases phenotypic hallmarks of aging, being a paradigm of rejuvenation. There is evidence for RS and inflammatory responses being barriers to efficient reprogramming (Ruiz et al., 2015; Soria-Valles et al., 2015). Given that calcitriol improves RS and aging phenotypes in HGPS cells, we tested its effect on reprogramming. HGPS fibroblasts were treated with calcitriol for 7 days and transduced with the "Yamanaka" factor cocktail OSKM (Oct4/Sox2/Klf4/Myc). We found that calcitriol increased significantly the efficiency of reprogramming into iPSCs compared with untreated cells (Figure 4F). This indicates that calcitriol "rejuvenates" HGPS cells and that amelioration of RS and repression of the STAT1/IFN-like response might contribute to its rejuvenating effect.

DISCUSSION

Our study shows that progerin expression causes RF stalling and nuclease-mediated degradation of the stalled forks. Given that DNA replication is the major source of spontaneous DNA double-strand breaks in dividing cells (Berti and Vindigni, 2016), progerin-induced RS could be a major cause of DNA damage in

(B) Heatmap shows the Gene Ontology (GO) analysis performed with the differential gene expression analysis (FC > 1.5 and < 0.6 and $p \leq 0.05$) between HGPS/NF and HGPScalcitriol/vehicle using DAVID and STRING.
(C) Heatmap shows differential expression (upregulation) of ~50 genes in the IFN/antiviral/innate immunity pathway between HGPS/NF and a decrease in HGPScalcitriol/vehicle.
(D) NF and HGPS fibroblasts were processed for immunofluorescence with antibodies recognizing STAT1 and active P-STAT1^{Y701} and nuclei stained with DAPI.
(E) Total cell lysates from untreated NFs and HGPS fibroblasts treated with vehicle or calcitriol for 4 days were processed for immunoblotting to monitor global levels of progerin, STAT1, and P-STAT1^{Y701}. β-Tubulin was used as loading control.
(F) Untreated NFs and HGPS cells treated with calcitriol or vehicle for 4 days were subjected to subcellular fractionation to monitor localization of P-STAT1^{Y701} and IRFs. Note the nuclear accumulation of P-STAT1 and IRF3 in HGPS cells and how calcitriol reduces their nuclear levels (red square).
(G) Graph shows mean densitometry analysis (a.u.) of immunoblots from (E) and (F).
* denotes p value of statistical significance (*$p < 0.05$, **$p < 0.01$, ***$p < 0.005$, and ****$p < 0.001$). Error bars represent SEM.

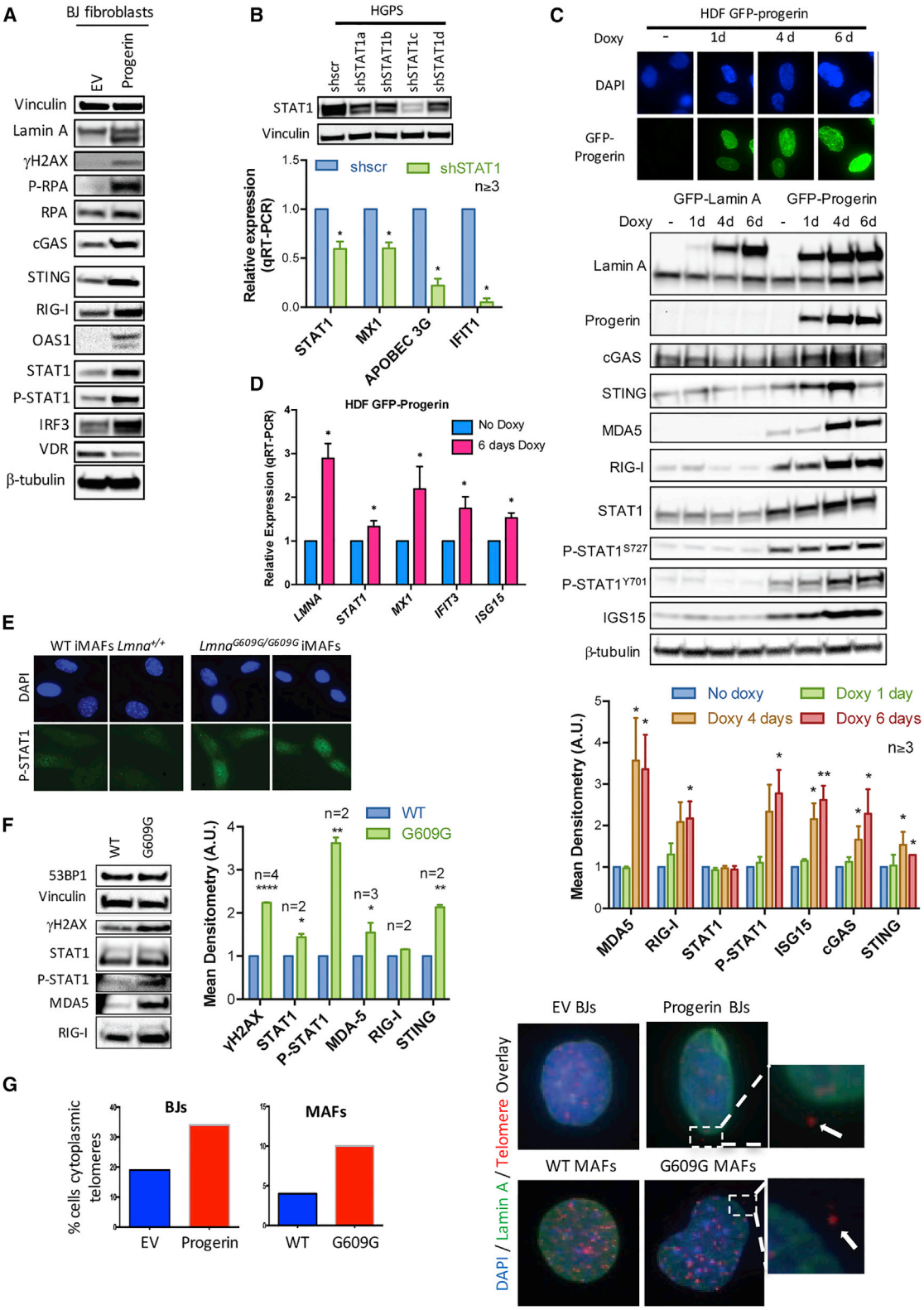

(legend on next page)

HGPS cells. RS is accompanied by the activation of a robust cell-intrinsic IFN-like response regulated by STAT1, which contributes to cellular decline in progeria. As such, compounds known to improve HGPS cell phenotypes, especially calcitriol, rescue RS, repress the STAT1/IFN-like response, and increase efficiency of reprogramming of HGPS cells, a paradigm of rejuvenation. Our study reveals molecular mechanisms underlying progerin toxicity and evidence for the broad benefits of calcitriol ameliorating aging phenotypes, suggesting that its use in preclinical models of progeria should be investigated.

IFN/inflammatory responses are activated in other syndromes of genomic instability and accelerated aging, such as ataxia telangiectasia (AT) and Fanconi anemia (FA) (Brégnard et al., 2016; Härtlova et al., 2015), and in telomerase KO mice (Yu et al., 2015). However, we find a fundamental difference between the activation of this pathway in HGPS and other syndromes, namely, the lack of expression of IFNs themselves. This suggests that the STAT1-mediated IFN-like response identified in HGPS is activated via cell-intrinsic non-canonical pathways that are independent of IFNs. IFN-independent activation of STAT1 by p38-MAPK, RIG-I, and Toll-like receptors (TLRs) has been reported in response to different stresses (Dempoya et al., 2012; Luu et al., 2014). These pathways could contribute to STAT1 activation in HGPS cells. Our results are consistent with studies monitoring markers of inflammation in urine and plasma samples from HGPS patients, which do not show increased levels of IFNs or a robust upregulation of inflammatory molecules compared with healthy age- and sex-matched controls (Gordon et al., 2018). These findings suggest that a cell-intrinsic IFN-like response is activated in HGPS patients' cells that contribute to cellular aging without an overt release of inflammatory molecules that alert the immune system. Alternatively, progerin might activate inflammation locally, for example in cells from the cardiovascular system, contributing to atherosclerosis in patients.

In addition to the STAT1/IFN-like response identified here, other studies showed an elevated NF-κB transcriptional profile in cellular and mouse models of HGPS, which is linked to the DNA damage response (Osorio et al., 2012). Inhibition of NF-κB slows aging and increases longevity of progeria mice and improves reprogramming of HGPS cells (Soria-Valles et al., 2015). We propose a model whereby RS and DNA damage are sensed by cytoplasmic PRRs, including cGAS/STING cytoplasmic DNA sensors, leading to activation of both NF-κB and STAT1 pathways, which cooperate promoting cellular aging.

EXPERIMENTAL PROCEDURES

Cell Culture

Skin fibroblasts from four HGPS patients and three parents were obtained from the Progeria Research Foundation (Supplemental Experimental Procedures). MAFs were isolated from the ears of *Lmna*$^{G609G/G609G}$ and wild-type mice and immortalized with SV40-LT. All cells were maintained in DMEM, 10% fetal bovine serum (FBS), antibiotics, and antimycotics. The Gonzalo laboratory is approved for animal use.

Calcitriol Treatment

Cells were supplemented as described (Kreienkamp et al., 2016).

Other Treatments

Cells were treated for 10 days with ATRA (100 nM), remodelin (1 μM), or a combination of lonafarnib (2 μM) and rapamycin (0.68 μM). Media with drugs was replenished either daily (lonafarnib and rapamycin) or every 3 days (ATRA, remodelin, calcitriol).

Progerin- and Lamin A-Inducible Cell Lines

HDFs containing doxycycline-inducible progerin or lamin A constructs were treated as described (Kubben et al., 2016).

Immuno-FISH

Cells growing in coverslips were first processed for immunofluorescence with anti-lamin A antibody, followed by processing for FISH. Cells were fixed in 3.7% paraformaldehyde/PBS for 10 min at room temperature (RT), washed in PBS, dehydrated in ethanol (70%, 90%, 100% ethanol), and air-dried. Hybridization solution containing the cy3-labeled telomeric probe was added to coverslips, which were heated to 80°C for 10 min and incubated for 3 hr at RT. Coverslips were washed twice for 15 min in washing solution and three times in PBS and stained with DAPI.

Viral Transduction

Retroviral and lentiviral transductions were performed as previously described (Gonzalez-Suarez and Gonzalo, 2010). Viral envelope and packaging plasmids were gifts from Sheila Stewart (Washington University School of Medicine [WUSM]), progerin-expressing plasmid was a gift from Brian Kennedy (Buck Institute), and shRNAs targeting STAT1 were purchased from Sigma-Aldrich.

Figure 3. Activation of PRRs, STAT1, and ISGs by Progerin

(A) Total cell lysates from BJs transduced with progerin or EV and processed for immunoblotting to detect lamin A (upper band) and progerin (lower band), DNA damage (γH2AX), RS (P-RPA), PRRs (cGAS, STING, RIG-I, OAS1), and PRR effectors (STAT1, IRF3). Vinculin was used as loading control. Densitometry analysis shown in Figure S1.

(B) HGPS fibroblasts were lentivirally transduced with four independent shRNAs targeting STAT1 (shSTAT1) and shRNA control (shscr). After selection of infected cells, levels of STAT1 protein were monitored by immunoblotting, and the levels of transcripts for *STAT1* and STAT1-regulated ISGs (*MX1*, *APOBEC3G*, *IFIT1*) by qRT-PCR. Graph shows average ± SEM of three or more independent experiments.

(C) HDFs were treated with doxycycline for increasing time periods (1–6 days). Fluorescence microscopy shows expression of GFP-progerin. Immunoblots show levels of different lamin A forms: endogenous lamin A (lower band), GFP-lamin A (upper band), GFP-progerin (middle band), PRRs (cGAS, STING, MDA5, RIG-I), STAT1 and P-STAT1 (Y701 and S727), ISG15, and progerin. β-Tubulin was used as loading control. Graph shows densitometry analysis in three or more biological repeats.

(D) RNA was extracted from progerin-expressing cells after 6 days in doxycycline, and the levels of total *LMNA* gene transcripts and transcripts of STAT1-regulated ISGs (*MX1*, *IFIT3*, *ISG15*) were monitored by qRT-PCR. Graph shows average ± SEM of three independent experiments.

(E) MAFs were isolated from *Lmna*$^{G609G/G609G}$ mice and wild-type (WT) littermates and immortalized with SV40-LT. Immunofluorescence with P-STAT1 antibody shows increased nuclear STAT1 in G609G iMAFs compared with WT controls.

(F) iMAFs were processed for immunoblotting to monitor levels of γH2AX, STAT1, P-STAT1, and PRRs (MDA5, RIG-I). Graph shows mean densitometry analysis of immunoblots ($n \geq 2$).

(G) BJ fibroblasts expressing progerin or EV and G609G and WT iMAFs were processed for immuno-FISH with a telomeric probe and lamin A antibody. The percentage of cells with telomeric DNA outside the nucleus was quantitated.

* denotes p value of statistical significance (*$p < 0.05$, **$p < 0.01$, ***$p < 0.005$, and ****$p < 0.001$). Error bars represent SEM.

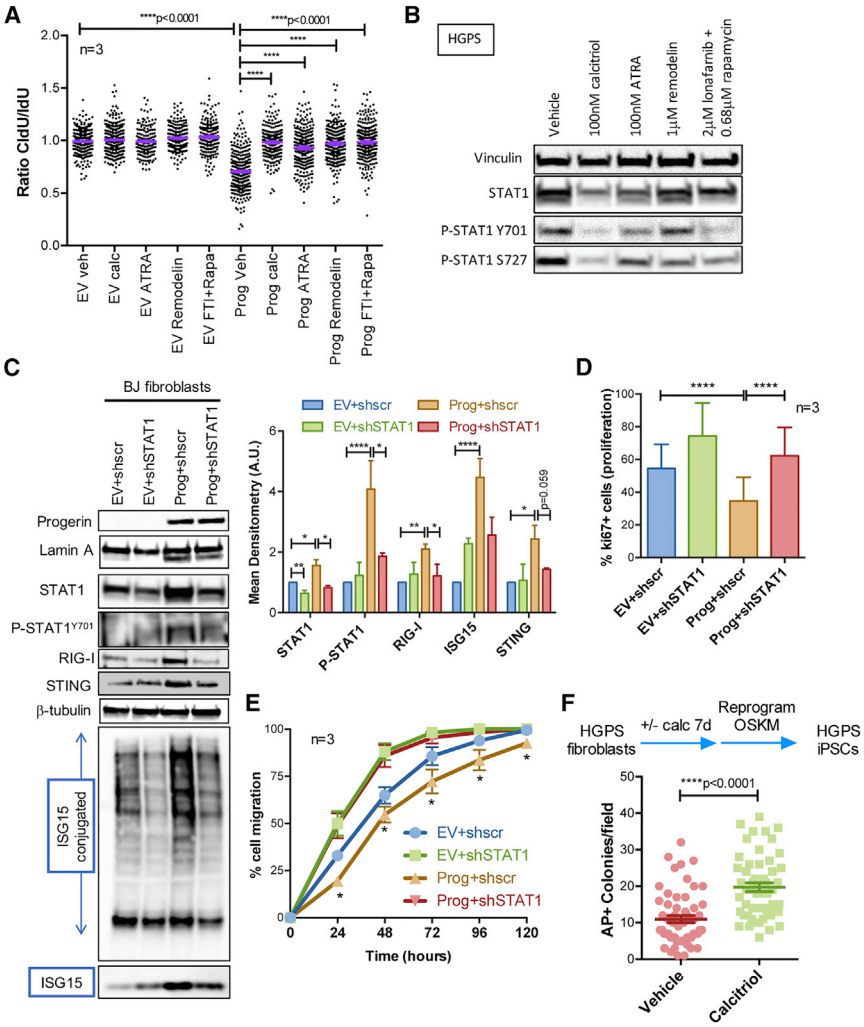

Figure 4. RS and the STAT1/IFN-like Response Underlie HGPS Cellular Decline

(A) RPE cells expressing progerin or EV were treated with vehicle, calcitriol (100 nM), ATRA (100nM), remodelin (1 μM), or a combination of lonafarnib (2 μM) and rapamycin (0.68 μM) for 10 days. DNA fiber assays were performed with the labeling scheme IdU for 25 min + CldU for 25 min. Graph shows the average ratio CldU/IdU in three biological repeats.

(B) HGPS fibroblasts subjected to the same treatment as in (A) were processed for immunoblotting to monitor levels of STAT1 and P-STAT1 on Y701 and S727. Vinculin was used as loading control.

(C) BJ fibroblasts expressing progerin or EV were lentivirally transduced with shRNA targeting STAT1 or shscr control. Immunoblots show levels of lamin A, progerin, STAT1, P-STAT1, PRRs (RIG-I and STING), and ISG15 (both conjugated and free). β-Tubulin was the loading control. Graph shows mean densitometry analysis of immunoblots ($n \geq 2$).

(D) The four lines generated in (C) were processed for immunofluorescence with Ki67 antibody to quantitate percentage of proliferating cells. Graph shows average ± SEM of three biological repeats.

(E) The four lines generated in (C) were subjected to a wound closure assay to monitor cell migration. Graph shows average ± SEM of three biological repeats, each performed in quadruplicate.

(F) HGPS fibroblasts were treated with calcitriol or vehicle for 7 days, and reprogramming was initiated via viral transduction of OSKM. Colonies of iPSCs were stained with alkaline phosphatase 2 weeks after transduction and counted.

* denotes p value of statistical significance (*$p < 0.05$, **$p < 0.01$, ***$p < 0.005$, and ****$p < 0.001$). Error bars represent SEM.

Proliferation and Wound Closure Assays

BJ fibroblasts expressing progerin or not, and transduced with shSTAT1 or shscr, were seeded on coverslips (3×10^5 cells/plate). Ki67 immunofluorescence was performed and images analyzed by counting the number of Ki67-positive cells with respect to total nuclei stained with DAPI. The four cell lines were also analyzed for migration in a wound closure assay. Cells were seeded in 48-well plates, and after ON incubation the culture was scratched with a sterile tip to produce a cell-free space (wound). Closure of the space by cells (wound closure) was recorded taking snapshot pictures at different time points (24–120 hr) and analyzing the cell-free area using ImageJ software (NIH). The rate of closure of the wound is an indication of cell migration.

Reprogramming

HGPS fibroblasts were treated with calcitriol or vehicle for 7 days. Cells were then infected using the CytoTune-iPS 2.0 Sendai reprogramming kit, which increased proliferation. After 7 days, 10^5 cells were seeded onto inactivated MEF feeders and medium replaced with hES medium every day. Cells were grown until hES-like colonies with a proper morphology emerged (~14 days). Colonies were stained with alkaline phosphatase and counted.

Statistical Analysis

For all qRT-PCR experiments, densitometry analysis, and reprogramming experiments, a standard "two-tailed" Student's t test was used to calculate statistical significance of the observed differences. For DNA fiber experiments, unpaired two-tailed t tests with Welch correction for unequal distribution were performed. We used GraphPad Prism software for all statistical analyses. In all cases, differences were considered statistically significant when $p < 0.05$.

Further details and an outline of resources used in this work can be found in Supplemental Experimental Procedures.

DATA AND SOFTWARE AVAILABILITY

The accession number for the RNA-seq files reported in this paper is GEO: GSE97986.

SUPPLEMENTAL INFORMATION

Supplemental Information includes Supplemental Experimental Procedures, one figure, and one table and can be found with this article online at https://doi.org/10.1016/j.celrep.2018.01.090.

ACKNOWLEDGMENTS

Jennifer Dulle participated in early stages of the project; Rajeev Aurora (St. Louis University), Tom Misteli (NIH), and Jason Weber (WUSM) provided insightful discussions and sharing reagents; Carlos Lopez-Otin (Oviedo)

provided the mice. Research in the laboratory of S. Gonzalo was supported by National Institute of General Medical Sciences (NIGMS) grant RO1 GM094513-01, U.S. Department of Defense (DOD) Breast Cancer Research Program (BCRP) Idea Award BC110089, and an SIP grant from the Siteman Cancer Center (SCC) 8074-88. R.K. was supported by an American Heart Association (AHA) predoctoral fellowship (16PRE27510016); and S. Graziano by an SCC pre-doctoral fellowship. A.V. was supported by NIH grant R01GM108648 and DOD BRCP Breakthrough Award BC151728. N.K. was supported by the Intramural Research Program of the NIH, National Cancer Institute (NCI), Center for Cancer Research.

AUTHOR CONTRIBUTIONS

R.K., S. Graziano, and N.C.-B. generated most of the data. G.B.-D. and E.C. performed some experiments. D.D. performed the RNA-seq analyses. L.F.Z.B. and A.V. provided guidance on reprogramming and replication studies, respectively. N.K. provided the HDF-progerin cell line and insightful discussions. S. Gonzalo supervised the research and prepared the manuscript. All authors read the manuscript and agreed to submit.

DECLARATION OF INTERESTS

The authors declare no conflict of interest.

Received: October 13, 2017
Revised: December 22, 2017
Accepted: January 30, 2018
Published: February 20, 2018

REFERENCES

Ahn, J., Xia, T., Konno, H., Konno, K., Ruiz, P., and Barber, G.N. (2014). Inflammation-driven carcinogenesis is mediated through STING. Nat. Commun. *5*, 5166.

Berti, M., and Vindigni, A. (2016). Replication stress: getting back on track. Nat. Struct. Mol. Biol. *23*, 103–109.

Bhattacharya, S., Srinivasan, K., Abdisalaam, S., Su, F., Raj, P., Dozmorov, I., Mishra, R., Wakeland, E.K., Ghose, S., Mukherjee, S., and Asaithamby, A. (2017). RAD51 interconnects between DNA replication, DNA repair and immunity. Nucleic Acids Res. *45*, 4590–4605.

Brégnard, C., Guerra, J., Déjardin, S., Passalacqua, F., Benkirane, M., and Laguette, N. (2016). Upregulated LINE-1 activity in the Fanconi anemia cancer susceptibility syndrome leads to spontaneous pro-inflammatory cytokine production. EBioMedicine *8*, 184–194.

Brzostek-Racine, S., Gordon, C., Van Scoy, S., and Reich, N.C. (2011). The DNA damage response induces IFN. J. Immunol. *187*, 5336–5345.

Cao, K., Blair, C.D., Faddah, D.A., Kieckhaefer, J.E., Olive, M., Erdos, M.R., Nabel, E.G., and Collins, F.S. (2011a). Progerin and telomere dysfunction collaborate to trigger cellular senescence in normal human fibroblasts. J. Clin. Invest. *121*, 2833–2844.

Cao, K., Graziotto, J.J., Blair, C.D., Mazzulli, J.R., Erdos, M.R., Krainc, D., and Collins, F.S. (2011b). Rapamycin reverses cellular phenotypes and enhances mutant protein clearance in Hutchinson-Gilford progeria syndrome cells. Sci. Transl. Med. *3*, 89ra58.

Chojnowski, A., Ong, P.F., Wong, E.S., Lim, J.S., Mutalif, R.A., Navasankari, R., Dutta, B., Yang, H., Liow, Y.Y., Sze, S.K., et al. (2015). Progerin reduces LAP2α-telomere association in Hutchinson-Gilford progeria. eLife *4*, 4.

Cobb, A.M., Murray, T.V., Warren, D.T., Liu, Y., and Shanahan, C.M. (2016). Disruption of PCNA-lamins A/C interactions by prelamin A induces DNA replication fork stalling. Nucleus *7*, 498–511.

Collins, F.S. (2016). Seeking a cure for one of the rarest diseases: progeria. Circulation *134*, 126–129.

Csoka, A.B., English, S.B., Simkevich, C.P., Ginzinger, D.G., Butte, A.J., Schatten, G.P., Rothman, F.G., and Sedivy, J.M. (2004). Genome-scale expression profiling of Hutchinson-Gilford progeria syndrome reveals widespread transcriptional misregulation leading to mesodermal/mesenchymal defects and accelerated atherosclerosis. Aging Cell *3*, 235–243.

Dempoya, J., Matsumiya, T., Imaizumi, T., Hayakari, R., Xing, F., Yoshida, H., Okumura, K., and Satoh, K. (2012). Double-stranded RNA induces biphasic STAT1 phosphorylation by both type I interferon (IFN)-dependent and type I IFN-independent pathways. J. Virol. *86*, 12760–12769.

Gonzalez-Suarez, I., and Gonzalo, S. (2010). Nurturing the genome: A-type lamins preserve genomic stability. Nucleus *1*, 129–135.

Gonzalo, S., and Kreienkamp, R. (2015). DNA repair defects and genome instability in Hutchinson-Gilford Progeria Syndrome. Curr. Opin. Cell Biol. *34*, 75–83.

Gonzalo, S., Kreienkamp, R., and Askjaer, P. (2016). Hutchinson-Gilford progeria syndrome: a premature aging disease caused by LMNA gene mutations. Ageing Res. Rev. *33*, 18–29.

Gordon, L.B., Rothman, F.G., López-Otín, C., and Misteli, T. (2014). Progeria: a paradigm for translational medicine. Cell *156*, 400–407.

Gordon, L.B., Kleinman, M.E., Massaro, J., D'Agostino, R.B., Sr., Shappell, H., Gerhard-Herman, M., Smoot, L.B., Gordon, C.M., Cleveland, R.H., Nazarian, A., et al. (2016). Clinical trial of the protein farnesylation inhibitors lonafarnib, pravastatin, and zoledronic acid in children with Hutchinson-Gilford progeria syndrome. Circulation *134*, 114–125.

Gordon, L.B., Campbell, S.E., Massaro, J.M., D'Agostino, R.B., Sr., Kleinman, M.E., Kieran, M.W., and Moses, M.A. (2018). Survey of plasma proteins in children with progeria pre-therapy and on-therapy with lonafarnib. Pediatr. Res. Published online January 17, 2018. https://doi.org/10.1038/pr.2018.9.

Härtlova, A., Erttmann, S.F., Raffi, F.A., Schmalz, A.M., Resch, U., Anugula, S., Lienenklaus, S., Nilsson, L.M., Kröger, A., Nilsson, J.A., et al. (2015). DNA damage primes the type I interferon system via the cytosolic DNA sensor STING to promote anti-microbial innate immunity. Immunity *42*, 332–343.

Hilton, B.A., Liu, J., Cartwright, B.M., Liu, Y., Breitman, M., Wang, Y., Jones, R., Tang, H., Rusinol, A., Musich, P.R., and Zou, Y. (2017). Progerin sequestration of PCNA promotes replication fork collapse and mislocalization of XPA in laminopathy-related progeroid syndromes. FASEB J. *31*, 3882–3893.

Kreienkamp, R., Croke, M., Neumann, M.A., Bedia-Diaz, G., Graziano, S., Dusso, A., Dorsett, D., Carlberg, C., and Gonzalo, S. (2016). Vitamin D receptor signaling improves Hutchinson-Gilford progeria syndrome cellular phenotypes. Oncotarget *7*, 30018–30031.

Kubben, N., Brimacombe, K.R., Donegan, M., Li, Z., and Misteli, T. (2015). A high-content imaging-based screening pipeline for the systematic identification of anti-progeroid compounds. Methods *96*, 46–58.

Kubben, N., Zhang, W., Wang, L., Voss, T.C., Yang, J., Qu, J., Liu, G.H., and Misteli, T. (2016). Repression of the antioxidant NRF2 pathway in premature aging. Cell *165*, 1361–1374.

Larrieu, D., Britton, S., Demir, M., Rodriguez, R., and Jackson, S.P. (2014). Chemical inhibition of NAT10 corrects defects of laminopathic cells. Science *344*, 527–532.

Liu, G.H., Barkho, B.Z., Ruiz, S., Diep, D., Qu, J., Yang, S.L., Panopoulos, A.D., Suzuki, K., Kurian, L., Walsh, C., et al. (2011). Recapitulation of premature ageing with iPSCs from Hutchinson-Gilford progeria syndrome. Nature *472*, 221–225.

Luu, K., Greenhill, C.J., Majoros, A., Decker, T., Jenkins, B.J., and Mansell, A. (2014). STAT1 plays a role in TLR signal transduction and inflammatory responses. Immunol. Cell Biol. *92*, 761–769.

Mackenzie, K.J., Carroll, P., Martin, C.A., Murina, O., Fluteau, A., Simpson, D.J., Olova, N., Sutcliffe, H., Rainger, J.K., Leitch, A., et al. (2017). cGAS surveillance of micronuclei links genome instability to innate immunity. Nature *548*, 461–465.

Midgley, A.C., Morris, G., Phillips, A.O., and Steadman, R. (2016). 17β-estradiol ameliorates age-associated loss of fibroblast function by attenuating IFN-γ/STAT1-dependent miR-7 upregulation. Aging Cell *15*, 531–541.

Murphy, A.K., Fitzgerald, M., Ro, T., Kim, J.H., Rabinowitsch, A.I., Chowdhury, D., Schildkraut, C.L., and Borowiec, J.A. (2014). Phosphorylated RPA recruits

PALB2 to stalled DNA replication forks to facilitate fork recovery. J. Cell Biol. *206*, 493–507.

Osorio, F.G., Bárcena, C., Soria-Valles, C., Ramsay, A.J., de Carlos, F., Cobo, J., Fueyo, A., Freije, J.M., and López-Otín, C. (2012). Nuclear lamina defects cause ATM-dependent NF-κB activation and link accelerated aging to a systemic inflammatory response. Genes Dev. *26*, 2311–2324.

Pellegrini, C., Columbaro, M., Capanni, C., D'Apice, M.R., Cavallo, C., Murdocca, M., Lattanzi, G., and Squarzoni, S. (2015). All-trans retinoic acid and rapamycin normalize Hutchinson Gilford progeria fibroblast phenotype. Oncotarget *6*, 29914–29928.

Pereira, S., Bourgeois, P., Navarro, C., Esteves-Vieira, V., Cau, P., De Sandre-Giovannoli, A., and Lévy, N. (2008). HGPS and related premature aging disorders: from genomic identification to the first therapeutic approaches. Mech. Ageing Dev. *129*, 449–459.

Ruiz, S., Lopez-Contreras, A.J., Gabut, M., Marion, R.M., Gutierrez-Martinez, P., Bua, S., Ramirez, O., Olalde, I., Rodrigo-Perez, S., Li, H., et al. (2015). Limiting replication stress during somatic cell reprogramming reduces genomic instability in induced pluripotent stem cells. Nat. Commun. *6*, 8036.

Scaffidi, P., and Misteli, T. (2008). Lamin A-dependent misregulation of adult stem cells associated with accelerated ageing. Nat. Cell Biol. *10*, 452–459.

Schlacher, K., Christ, N., Siaud, N., Egashira, A., Wu, H., and Jasin, M. (2011). Double-strand break repair-independent role for BRCA2 in blocking stalled replication fork degradation by MRE11. Cell *145*, 529–542.

Singh, M., Hunt, C.R., Pandita, R.K., Kumar, R., Yang, C.R., Horikoshi, N., Bachoo, R., Serag, S., Story, M.D., Shay, J.W., et al. (2013). Lamin A/C depletion enhances DNA damage-induced stalled replication fork arrest. Mol. Cell. Biol. *33*, 1210–1222.

Soria-Valles, C., Osorio, F.G., Gutiérrez-Fernández, A., De Los Angeles, A., Bueno, C., Menéndez, P., Martín-Subero, J.I., Daley, G.Q., Freije, J.M., and López-Otín, C. (2015). NF-κB activation impairs somatic cell reprogramming in ageing. Nat. Cell Biol. *17*, 1004–1013.

Swift, J., Ivanovska, I.L., Buxboim, A., Harada, T., Dingal, P.C., Pinter, J., Pajerowski, J.D., Spinler, K.R., Shin, J.W., Tewari, M., et al. (2013). Nuclear lamin-A scales with tissue stiffness and enhances matrix-directed differentiation. Science *341*, 1240104.

Szelag, M., Piaszyk-Borychowska, A., Plens-Galaska, M., Wesoly, J., and Bluyssen, H.A. (2016). Targeted inhibition of STATs and IRFs as a potential treatment strategy in cardiovascular disease. Oncotarget *7*, 48788–48812.

van Steensel, B., and Belmont, A.S. (2017). Lamina-associated domains: links with chromosome architecture, heterochromatin, and gene repression. Cell *169*, 780–791.

Vincent, J., Adura, C., Gao, P., Luz, A., Lama, L., Asano, Y., Okamoto, R., Imaeda, T., Aida, J., Rothamel, K., et al. (2017). Small molecule inhibition of cGAS reduces interferon expression in primary macrophages from autoimmune mice. Nat. Commun. *8*, 750.

Wang, H., Hu, S., Chen, X., Shi, H., Chen, C., Sun, L., and Chen, Z.J. (2017). cGAS is essential for the antitumor effect of immune checkpoint blockade. Proc. Natl. Acad. Sci. U S A *114*, 1637–1642.

Wheaton, K., Campuzano, D., Ma, W., Sheinis, M., Ho, B., Brown, G.W., and Benchimol, S. (2017). Progerin-induced replication stress facilitates premature senescence in Hutchinson-Gilford progeria syndrome. Mol. Cell. Biol. *37*, 37.

Wolf, C., Rapp, A., Berndt, N., Staroske, W., Schuster, M., Dobrick-Mattheuer, M., Kretschmer, S., König, N., Kurth, T., Wieczorek, D., et al. (2016). RPA and Rad51 constitute a cell intrinsic mechanism to protect the cytosol from self DNA. Nat. Commun. *7*, 11752.

Yang, H., Wang, H., Ren, J., Chen, Q., and Chen, Z.J. (2017). cGAS is essential for cellular senescence. Proc. Natl. Acad. Sci. U S A *114*, E4612–E4620.

Yu, Q., Katlinskaya, Y.V., Carbone, C.J., Zhao, B., Katlinski, K.V., Zheng, H., Guha, M., Li, N., Chen, Q., Yang, T., et al. (2015). DNA-damage-induced type I interferon promotes senescence and inhibits stem cell function. Cell Rep. *11*, 785–797.

Zhang, J., Lian, Q., Zhu, G., Zhou, F., Sui, L., Tan, C., Mutalif, R.A., Navasankari, R., Zhang, Y., Tse, H.F., et al. (2011). A human iPSC model of Hutchinson Gilford progeria reveals vascular smooth muscle and mesenchymal stem cell defects. Cell Stem Cell *8*, 31–45.

Cell Reports, Volume *22*

Supplemental Information

A Cell-Intrinsic Interferon-like Response Links Replication Stress to Cellular Aging Caused by Progerin

Ray Kreienkamp, Simona Graziano, Nuria Coll-Bonfill, Gonzalo Bedia-Diaz, Emily Cybulla, Alessandro Vindigni, Dale Dorsett, Nard Kubben, Luis Francisco Zirnberger Batista, and Susana Gonzalo

Supplemental experimental procedures

Immunoblotting and Immunofluorescence

Immunoblotting. Cells were lysed in UREA buffer (8 M Urea, 40 mM Tris pH7.5, 1% NP40) for 20 minutes on ice, and 60-120 µg of total protein was loaded on 4-15% Criterion-TGX-Gel (Bio-Rad). Subcellular fractionation was performed using a fractionation kit (Thermo, 78840). We started with an equal number of cells, and an equal volume of lysate was loaded for westerns. Densitometry analysis was performed using Image-J software.

Immunofluorescence. $3x10^5$ cells were fixed in 3.7% formaldehyde+0.2% Triton-X100 in PBS for 10 minutes, washed 3X in PBS, and blocked 1 hour at 37°C in 10% BSA/PBS. Incubations with antibodies were performed for 1 hour at 37°C, in a humid chamber. After washes in PBS, cells were counterstained with DAPI in Vectashield. Microscopy and photo capture was performed on a Leica DM5000 B microscope using 40x or 63x oil objective lenses with a Leica DFC350FX digital camera and the Leica Application Suite.

Quantitative Reverse-Transcription PCR

cDNA was generated by reverse transcription of 1 µg total RNA using GeneAmp® RNA PCR kit. qRT-PCR was performed using the 7500HT Fast Real-Time PCR system with the Taqman® Universal PCR Master Mix or Universal SYBR Green Supermix. Reactions were carried out in triplicate and target gene and endogenous controls amplified in the same plate. Relative quantitative measurements of target genes were determined by comparing cycle thresholds. Table 3 in SI lists oligos used.

DNA Fiber Assays

Fiber assays were performed on retinal pigment epithelial cells (RPE cells) expressing EV or progerin. Asynchronous RPE cells were labeled for 25 min each with two thymidine analogs: 20 µM iododeoxyuridine (IdU) followed by 200 µM chlorodeoxyuridine (CIdU). Cells were collected by trypsinization, washed and resuspended in 100 µl of PBS. Then, 2 µl cell suspension was dropped on a polarized slide (Denville Ultraclear) and cell lysis was performed in situ by adding

8 µl of lysis buffer (200 mM Tris-HCl pH7.5; 50 mM EDTA; 0.5% SDS). Stretching of high-molecular weight DNA was achieved by tilting the slides at 15-45°. The resulting DNA spreads were air dried and fixed for 5 min in 3:1 Methanol:Acetic acid, and refrigerated overnight. For immunostaining, stretched DNA fibers were denatured with 2.5 N HCl for 60 min, washed 3X in PBS, then blocked with 5% BSA in PBS for 30 min at 37°C. Rat anti-CldU/BrdU (Abcam, ab6326) (1:100), chicken anti-rat Alexa 488 (Invitrogen, A21470) (1:100), mouse anti-IdU/BrdU (BD Biosciences, 347580) (1:20) and goat anti-mouse IgG1 Alexa 547 (Invitrogen, A21123) (1:100) antibodies were used to reveal CldU- and IdU-labeled tracts, respectively. A Leica SP5X confocal microscope was used to visualize the labeled tracts, and tract lengths were measured using ImageJ (http://rsbweb.nih.gov.beckerproxy.wustl.edu/ij/). Statistical analysis of the tract length was performed using GraphPad Prism (http://www.graphpad.com/scientific-software/prism/).

RNAseq

Normal and HGPS fibroblasts supplemented with 10^{-7} M calcitriol (1α,25-dihydroxyvitamin D_3; Sigma-Aldrich) or FBS for different periods of time (NF for 4 days and HGPS for 4 and 90 days) were utilized to extract total RNA using Aurum Total RNA Mini Kit (Bio-Rad) with DNaseI treatment following the manufacturer's protocol. Ribosomal RNA depletion was performed with 500 ng of total RNA with the Ribominus Eukaryotic System v2 (Life Technologies) according to the manufacturer's directions. The rRNA-depleted RNA was used to construct barcoded libraries using the Ion Total RNA-Seq Kit v2 (Life Technologies), following the manufacturer's instructions. The libraries were sequenced on an Ion Torrent Proton with a mean read length of ~100 nucleotides.

RNA-seq quantification was performed using a method similar to that described previously [1]. Sequencing reads were aligned to the hg19 genome sequence using the map4 algorithm in the TMAP aligner (https://github.com/iontorrent/TMAP/blob/master/doc/tmap-book.pdf), allowing soft clipping of both the 5' and 3' ends (option -g 0) and a minimum seed length of 20. The

resulting bam files were sorted using SAMtools [2] and used to generate strand-specific bedgraph files of the base pair coverage using BEDTools [3]. A custom R (R Core Team; http://www.R-project.org) script was used to convert the strand-specific bedgraph files to sgr files, which were used to sum the strand-specific base pair coverage of non-redundant sets of plus strand and minus strand exons using a custom R script. The nucleotide coverage values of all exons for each gene were summed using an R script to generate nucleotide coverage values for all annotated genes. The coverage values for each gene were normalized to the total coverage for all genes for each library to allow quantitative comparisons.

All RNA-seq files were submitted to the GEO repository, and the following accession number was assigned: GSE97986.

Gene Ontology analysis and heat-map generation

DAVID (http://david.niaid.nih.gov) bioinformatics resource was used to obtain functional interpretation of gene expression changes in HGPS compared to NF and in HGPS treated with calcitriol versus vehicle. We uploaded gene lists and via functional annotation clustering, we obtained gene-term enrichment analysis and biological mechanisms associated with the gene lists. We used gene-enrichment scores to generate heat-maps in order to represent biological data. Heat-maps were generated using a custom R script using the g-plots package. Values represent log2 values of relative gene expression as determined by RNA sequencing.

Resource Table

Cells (Skin fibroblasts) from Progeria Research Foundation	**Description**
HGPS2-HGADFN167	Fibroblasts from HGPS patient with classic mutation
HGADFN003	Fibroblasts from HGPS patient with classic mutation
HGPS3-PSADFN392	Fibroblasts from HGPS patient with non-classic mutation
PSADFN257	Fibroblasts from HGPS patient with non-classic mutation
PSFDFN327	Fibroblasts from parent of HGPS patient
HGMDFN090	Fibroblasts from parent of HGPS patient
PSMDFN346	Fibroblasts from parent of HGPS patient

Antibodies used for immunoblotting	**Antibody (Dilution)**
γH2AX	#2577, Cell Signaling (1:1000)
53BP1	sc-22760, SCBT (1:1000)
Lamin A	ab26300, Abcam (1:1000)
Progerin	SAB4200272, Sigma-Aldrich (1:1000)
Lamin A/C	sc-20681, SCBT (1:2000)
Vinculin	sc-7649, SCBT (1:1000)
VDR	sc-13133, SCBT (1:200)
β-Tubulin	T8238, Sigma Aldrich (1:2000)
STAT	#9172, Cell Signaling (1:1000)
P-STAT (Y701)	#7649, Cell Signaling (1:1000)
P-STAT (S727)	#9177, Cell Signaling (1:1000)
IRF3	#11904, Cell Signaling (1:1000)
P-RPA	A300-245A, Bethyl Laboratories (1:1000)
RPA	NA18, EMD Millipore (1:1000)
ISG15	sc-166755, SCBT (1:1000)
MDA5	#5321, Cell Signaling (1:1000)
RIG-I	#3743, Cell Signaling (1:1000)
cGAS	#D1D3G, Cell Signaling (1:300)
STING	#D2P2F, Cell Signaling (1:1000)

Antibodies used for immunofluorescence	**Antibody**
γH2AX	#2577, Cell Signaling
Lamin A	ab26300, Abcam
STAT	#9172, Cell Signaling
P-STAT (Y701)	#7649, Cell Signaling
P-STAT (S727)	#9177, Cell Signaling
Goat anti-Mouse and Goat anti-Rabbit Alexa Fluor 594/488-labeled secondary antibodies	Invitrogen

Primers used for SYBR Green qRT-PCR	Primers (5'-3')
18S (H)	F-GGTAACCCGTTGAACCCCATT
	R-CCATCCAATCGGTAGTAGCG
APOBEC3G (H)	F-GTCCTCTGACCCAAGGTTCA
	R-AGCACTGTTGGAGCAAGTTC
GAPDH (H)	F-GCATGGCCTTCGGTGTCC

	R-AATGCCAGCCCCAGCGTCAAA
IFITM1 (H)	F-CCAAGGTCCACCGTGATTAAC
	R-ACCAGTTCAAGAAGAGGGTGTT
LMNA (H)	F–GAGGAGGGCAAGTTTGTCCG
	R–CATTCTGGCGCTTGATCTGC
Lamin A Only (H)	F-GGACAATCTGGTCACCCGC
	R-GCGTCAGGAGCCCTGAGC
MX1 (H)	F-CTGCACAGGTTGTTCTCAGC
	R-GTTTCCGAAGTGGACATCGCA
Progerin (H)	F-GCGTCAGGAGCCCTGAGC
	R-GACGCAGGAAGCCTCCAC
STAT1 (H)	F-ATCAGGCTCAGTCGGGGAATA
	R-TGGTCTCGTGTTCTCTGTTCT
18S (M)	F-CATTCGAACGTCTGCCCTATC
	R-CCTGCTGCCTTCCTTGGA
Gapdh (M)	F-GTGCAGTGCCAGCCTCGTCC
	R-GCCACTGCAAATGGCAGCCC
Lmna (M)	F-ACCCCGCTGAGTACAACCT
	R-TTCGAGTGACTGTGACACTGG

References:

1. Wu, Y. *et al.* Drosophila Nipped-B Mutants Model Cornelia de Lange Syndrome in Growth and Behavior. *PLoS Genet* **11**, e1005655 (2015).
2. Li, H. *et al.* The Sequence Alignment/Map format and SAMtools. *Bioinformatics* **25**, 2078-2079 (2009).
3. Quinlan, A.R. & Hall, I.M. BEDTools: a flexible suite of utilities for comparing genomic features. *Bioinformatics* **26**, 841-842 (2010).

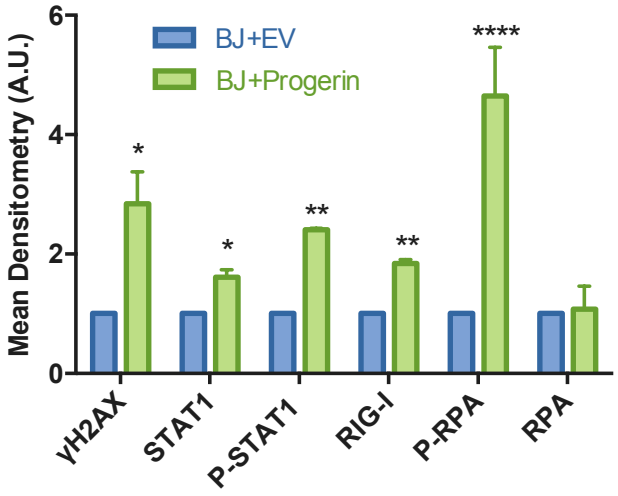

Figure S1. Related to Figure 3A; Replication stress and activation of STAT1 pathway upon progerin expression in normal cells. Total cell lysates from BJ fibroblasts expressing progerin or EV control were processed for immunoblotting and densitometry analysis performed in three biological repeats. Note the increased levels of DNA damage (γH2AX), replication stress (P-RPA), and STAT1 phosphorylation in progerin-expressing cells.